

REVIEW

On the importance of skewed offspring distributions and background selection in virus population genetics

KK Irwin^{1,2}, S Laurent^{1,2}, S Matuszewski^{1,2}, S Vuilleumier^{1,2}, L Ormond^{1,2}, H Shim^{1,2}, C Bank^{1,2,3} and JD Jensen^{1,2,4}

Many features of virus populations make them excellent candidates for population genetic study, including a very high rate of mutation, high levels of nucleotide diversity, exceptionally large census population sizes, and frequent positive selection. However, these attributes also mean that special care must be taken in population genetic inference. For example, highly skewed offspring distributions, frequent and severe population bottleneck events associated with infection and compartmentalization, and strong purifying selection all affect the distribution of genetic variation but are often not taken into account. Here, we draw particular attention to multiple-merger coalescent events and background selection, discuss potential misinference associated with these processes, and highlight potential avenues for better incorporating them into future population genetic analyses.

Heredity advance online publication, 21 September 2016; doi:10.1038/hdy.2016.58

INTRODUCTION

Viruses appear to be excellent candidates for studying evolution in real time; they have short generation times, high levels of diversity often driven by very large mutation rates and population sizes (both census and effective), and they experience frequent positive selection in response to host immunity or antiviral treatment. However, despite these desired attributes, standard population genetic models must be used with caution when making evolutionary inference.

First, population genetic inference is usually based on a coalescence model of the Kingman type, under the assumption of Poisson-shaped offspring distributions where the variance equals the mean and is always small relative to the population size; consequently, only two lineages may coalesce at a time. In contrast, viruses have highly variable reproductive rates, taken as rates of replication; these may vary based on cell or tissue type, level of cellular differentiation or stage in the lytic/lysogenic cycle (Knipe and Howley, 2007), resulting in highly skewed offspring distributions. This model violation is further intensified by the strong bottlenecks associated with infection and by strong positive selection (Neher and Hallatschek, 2013). Therefore, virus genealogies may be best characterized by *multiple-merger* coalescent (MMC) models (see, for example, Donnelly and Kurtz, 1999; Pitman, 1999; Sagitov, 1999; Schweinsberg, 2000; Möhle and Sagitov, 2001; Eldon and Wakeley, 2008), instead of the Kingman coalescent.

Second, the mutation rates of many viruses, particularly RNA viruses, are among the highest observed across taxa (Lauring *et al.*, 2013; Cuevas *et al.*, 2015). Although these high rates of mutation are what enables new beneficial mutations to arise, potentially allowing for rapid resistance to host immunity or antiviral drugs, they also render high mutational loads (Sanjuán, 2010; Lauring *et al.*, 2013). Specifically, the distribution of fitness effects has now been described across

taxa—demonstrating that the input of deleterious mutations far outnumbers the input of beneficial mutations (Acevedo *et al.*, 2014; Bank *et al.*, 2014; Bernet and Elena, 2015; Jiang *et al.*, 2016). The purging of these deleterious mutants through purifying selection can affect other areas in the genome through a process known as background selection (BGS) (Charlesworth *et al.*, 1993). Accounting for these effects is important for accurate evolutionary inference in general (Ewing and Jensen, 2016), but essential for the study of viruses because of their particularly high rates of mutation and compact genomes (Renzette *et al.*, 2016).

Given these distinctive features of virus populations and the increasing use of population genetic inference in this area (see, for example, Renzette *et al.*, 2013; Foll *et al.*, 2014; Pennings *et al.*, 2014; Renzette *et al.*, 2016), it is crucial to account for these processes that are shaping the amount and distribution of variation across their genomes. We aim here to draw particular attention to MMC events and background selection, and the repercussions of ignoring them in population genetic inference, highlighting particular applications to viruses. We conclude with general recommendations for how best to address these topics in the future.

SKewed OFFSPRING DISTRIBUTIONS AND THE MMC Inferring evolutionary history using the Wright–Fisher model: benefits and shortcomings

Many population genetic statistics and subsequent inference are based on the Kingman coalescent and the Wright–Fisher (WF) model (Wright, 1931; Kingman, 1982). With increasing computational power, the WF model has also been implemented in forward-time methods, allowing the modeling of more complex evolutionary scenarios versus backward-time methods. This also allows for the

¹École Polytechnique Fédérale de Lausanne (EPFL), School of Life Sciences, Lausanne, Switzerland; ²Swiss Institute of Bioinformatics (SIB), Lausanne, Switzerland; ³Instituto Gulbenkian de Ciência (IGC), Oeiras, Portugal and ⁴Arizona State University (ASU), School of Life Sciences, Center for Evolution & Medicine, Tempe, AZ, USA

Correspondence: Professor JD Jensen, Arizona State University, School of Life Sciences, Center for Evolution & Medicine, Tempe, AZ 85287, USA.

E-mail: Jeffrey.D.Jensen@asu.edu

Received 12 April 2016; accepted 8 June 2016

inference of population genetic parameters, including selection coefficients and effective population sizes (N_e), even from time-sampled data (that is, data collected at successive time points) (Ewens, 1979; Williamson and Slatkin, 1999; Malaspina *et al.*, 2012; Foll *et al.*, 2014; Foll *et al.*, 2015; Ferrer-Admetlla *et al.*, 2016; Malaspina, 2016). These methods are robust to some violations of WF model assumptions, such as constant population size, random mating, and non-overlapping generations, and have also been extended to accommodate selection, migration, and population structure (Neuhauser and Krone, 1997; Nordborg, 1997; Wilkinson-Herbots, 1998).

However, it has been suggested that violations of the assumption of a small variance in offspring number in the WF model, and in other models that result in the Kingman coalescent in the limit of large population size, lead to erroneous inference of population genetic parameters (Eldon and Wakeley, 2006). Biological factors such as sweepstake reproductive events, population bottlenecks, and recurrent positive selection may lead to skewed distributions in offspring number (Eldon and Wakeley, 2006; Li *et al.*, 2014); examples include various prokaryotes (plague), fungi (*Zymoseptoria tritici*, *Puccinia striiformis*, rusts, mildew, oomycetes), plants (*Arabidopsis thaliana*), marine organisms (sardines, cods, salmon, oysters), crustaceans (*Daphnia*) and insects (aphids) (reviewed in Tellier and Lemaire, 2014). The resulting skewed offspring distributions can also result in elevated linkage disequilibrium despite frequent recombination, as linkage depends not only on recombination rate, but also on the degree of skewness in offspring distributions (Eldon and Wakeley, 2008; Birkner *et al.*, 2013). Such events may also skew estimates of F_{ST} relative to those expected under WF models, as there is a high probability of alleles being *identical by descent* in subpopulations, where the expectation of coalescent times within subpopulations is less than that between subpopulations regardless of the timescale or magnitude of gene flow (Eldon and Wakeley, 2009).

The assumption of small variance in offspring number may often be violated in virus populations as well. For example, progeny RNA virus particles from infected cells can vary up to 100-fold (Zhu *et al.*, 2009). Second, features such as diploidy, recombination, and latent stages are expected to increase the probability of multiple-merger events (Davies *et al.*, 2007; Taylor and Véber, 2009; Birkner *et al.*, 2013). Third, within their life cycle, viruses experience bottleneck events during transmission and compartmentalization, followed by strong selective pressure from both the immune system and drug treatments. Finally, at the epidemic level, extinction–colonization dynamics drive population expansion (Anderson and May, 1991).

All of these aspects characterize, for example, HIV, a diploid virus with extraordinary rates of recombination (Schlub *et al.*, 2014). Transmitted and founder viruses undergo at least two distinct genetic bottlenecks (one at physical transmission and one at infection, respectively; Joseph and Swanstrom, 2015), followed by strong selection imposed by the immune system (Moore *et al.*, 2002). At the epidemic scale, besides multiple events of colonization (Tebit and Arts, 2011), strong heterogeneity in the virus transmission chain has also been observed (see, for example, Service and Blower, 1995).

Beyond WF assumptions: the MMC

A more general coalescent class of models, summarized as the MMC class, can account for these violations, particularly for (non-Poisson) skewed offspring distributions, by allowing more than two lineages to coalesce at a time (Table 1). These are often derived from Moran models (Moran, 1958), generalized to allow multiple offspring per individual. In contrast to the Kingman coalescent (for which $P(k > 2) = 0$, where k

Table 1 Hierarchy of coalescent models in decreasing order of generality

Coalescent model	Allows MMs?	Allows simultaneous MMs?	Distribution and parameters	References
Ξ -Coalescent	Yes	Yes	MMC events occur at rate λ , with a specific measure ξ on the infinite simplex and which allows an arbitrary number of simultaneous mergers.	Schweinsberg (2000); Möhle and Sagitov (2001)
Λ -Coalescent	Yes	No	MMC events occur at rate λ (but ≤ 1 event/time)	Donnelly and Kurtz (1999); Pitman (1999); Sagitov (1999)
Ψ -Coalescent	Yes	No	λ follows a distribution that depends on Ψ , that is., the fraction of the population replaced by the offspring of a single individual	Eldon and Wakeley (2006); Eldon and Wakeley (2008); Eldon and Wakeley (2009); Eldon and Degnan (2012)
Beta-coalescent	Yes	No	λ follows β -distribution: $\beta(\alpha, 2-\alpha)$ with $1 \leq \alpha < 2$	Schweinsberg (2003); Berestycki <i>et al.</i> (2007); Berestycki <i>et al.</i> (2008); Birkner and Blath (2008); Birkner <i>et al.</i> (2013); Steinrück <i>et al.</i> (2013)
Bolthausen-Sznitman	Yes	No	λ follows β -distribution with $\alpha = 1$: $\beta(1, 1) =$ uniform on $[0, 1]$	Bolthausen and Sznitman (1998); Basdevant and Goldschmidt (2008); Neher and Hallatschek (2013)
Kingman coalescent	No	No	λ follows β -distribution with $\alpha = 2$; Λ has unit mass at 0 ($\Lambda(dx) = \delta_0(dx)$)	Kingman (1982)

Abbreviations: MM, multiple merger; MMC, multiple-merger coalescent. Coalescent models listed in decreasing order with respect to generality.

is the number of lineages coalescing simultaneously), a probability distribution for k -merger events determines coalescence.

The parameters inferred under the MMC differ from those inferred under the Kingman coalescent in several notable respects. In the Kingman coalescent, effective size N_e scales linearly with census size N , whereas for the MMC it does not (Huillet and Möhle, 2011). Thus genetic diversity is a nonlinear function of population size. Coalescent trees under the MMC also have more pronounced star-like genealogies with longer branches (Figure 1), and their site frequency spectra (SFSs) are skewed toward an excess of low-frequency and high-frequency variants because of these branch lengths (Eldon and Wakeley, 2006; Blath *et al.*, 2016), generating a more negative Tajima's D (Birkner *et al.*, 2013). With similar migration and population size, alleles fix at a higher rate per population in the MMC than under the Kingman coalescent, and thus higher F_{ST} is expected between subpopulations (Eldon and Wakeley, 2009). Furthermore, the efficacy of selection increases, as selection acts almost deterministically between multiple-merger events; in the WF model, genetic drift counteracts selection fairly strongly (Der *et al.*, 2011), but in generalized models where offspring distributions are wide, beneficial mutations may be more likely to escape stochastic loss and thus continue to fixation. Furthermore, the fixation probability of a new mutant with a positive selection coefficient approaches 1 as the population size increases, in stark contrast with traditional expectations under the standard WF model (Der *et al.*, 2011).

Not accounting for skewed offspring distributions can lead to misinference. For instance, Eldon and Wakeley (2006) showed that for Pacific oysters, which have been argued to undergo sweepstake-like reproductive events (Hedgecock, 1994a), the estimated population-wide mutation rate θ inferred under the Kingman coalescent is two orders of magnitude larger than that obtained from the Ψ -coalescent

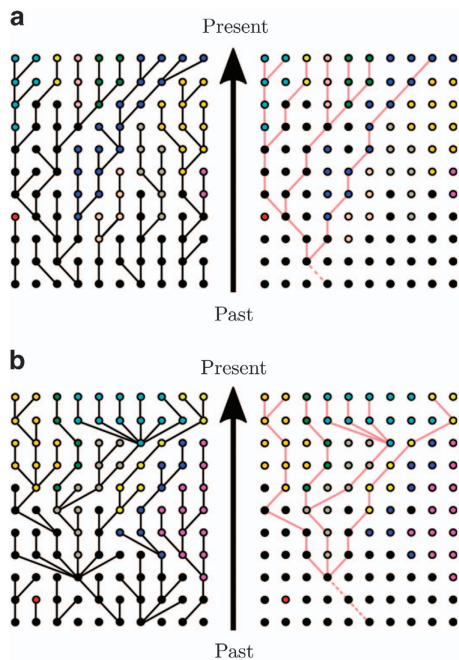


Figure 1 Multiple-merger and Kingman coalescent realizations. Example of genealogies and samples from (a) the Kingman coalescent and (b) a multiple-merger coalescent. Panels on the left show the evolutionary process of the whole population, whereas those on the right show a possible sampling and its resulting genealogy. Colors correspond to different (neutral) derived allelic states, where black denotes the wild type.

(see below)—9 vs 0.0308, respectively—and, indeed, provides a poor fit to the data.

The Ψ -coalescent

Introduced by Eldon and Wakeley (2006), the Ψ -coalescent (also called the ‘Dirac-coalescent’) differentiates two possible reproductive events in the underlying forward process (Figure 2). Either a standard Moran model reproduction event occurs (with probability $1 - \epsilon$), where a single individual is randomly chosen to reproduce and the (single) offspring replaces one randomly chosen nonparental individual; all other individuals, including the parent, persist. Alternatively, a ‘sweepstake’ reproductive event occurs (with probability ϵ) (Hedgecock, 1994b), where a single parent replaces Ψ^*N individuals. If these sweepstake events happen frequently enough, the rate of Ψ^*N -reproduction events will be much greater than that of two-reproduction events, and the underlying coalescent process will consequently be characterized by MM events; if two or more parents were to replace Ψ^*N individuals, simultaneous MM events may occur in a single generation resulting in a Ξ -coalescent. However, in contrast to other MMC models (for example, Ξ -coalescent or other Λ -coalescents), the parameter Ψ has a clear biological interpretation as the fraction of the population that is replaced in each sweepstake reproductive event. Though the assumption of a fixed Ψ (as in the normal Ψ -coalescent) seems biologically unrealistic, it can be avoided by treating Ψ as a Poisson parameter. Finally, despite its appealing connection to biologically relevant measures, the appropriateness of making inferences based on the Ψ -coalescent still depends on the biology of the specific virus being studied. Thus, model choice is still essential, and the best-fit coalescent should be assessed on a case-by-case basis.

Application to viruses

There are several reasons why a modified Moran model may better capture virus evolution than models converging to the Kingman coalescent, even though it does not account for fitness differences between individuals. First, virus evolution is driven by strong bottlenecks during host transmission and intrahost selection processes that likely result in skewed offspring distributions (Figure 3) (Gutiérrez *et al.*, 2012; Tellier and Lemaire, 2014). Furthermore, viruses display the MMC-typical low N_e/N ratio (Pennings *et al.*, 2014; Tellier and Lemaire, 2014), can adapt rapidly (Neher and Hallatschek, 2013), and may have sweepstake-like reproductive events in which a single virion can propagate a large fraction of the entire population (Grenfell *et al.*, 2004; Pybus and Rambaut, 2009). For example, the influenza virus hemagglutinin segment appears to be under strong directional selection imposed by host immunity (and sometimes drug treatment), resulting in a ladder-like genealogy (as depicted in Figure 3a), suggesting that only a few viruses seed the entire next generation (Grenfell *et al.*, 2004). That being said, some challenges remain (see Box 1), such

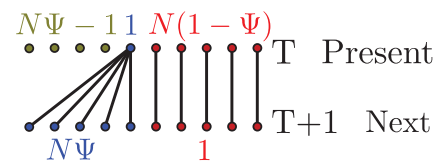


Figure 2 Depiction of the modified Moran model underlying the Ψ -coalescent. Lineages between the present and the next generation, where N is the population size, ϵ is the probability of a sweepstake event and Ψ is the fraction of the population that is replaced in each such event. Labels in the top row give the number of parental individuals reproducing in a given manner (represented by color), whereas labels in the bottom row give the number of corresponding offspring per parent.

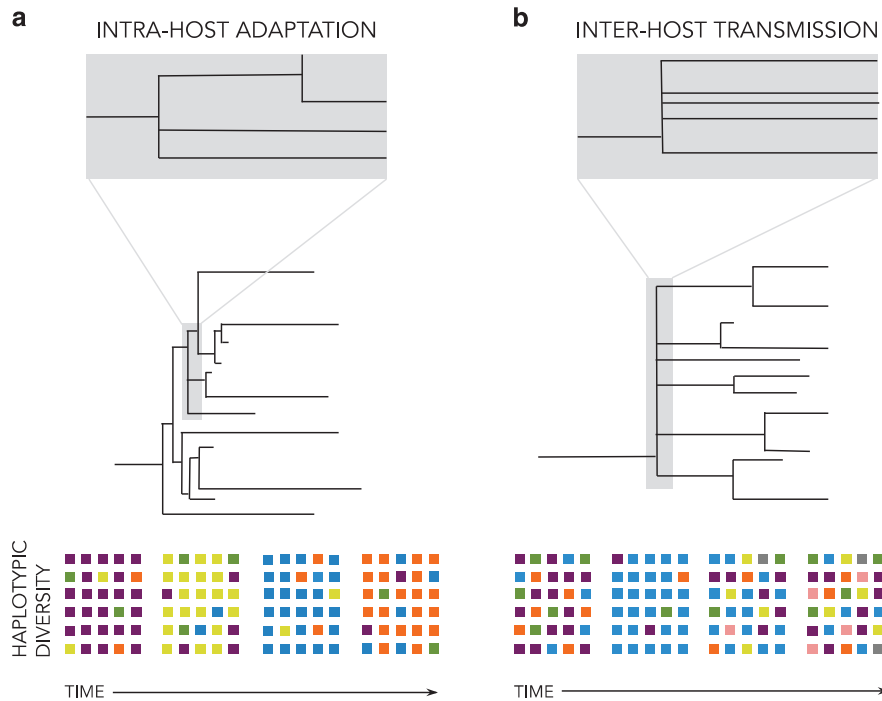


Figure 3 Example of processes spurring MM events in virus populations. Examples include (a) intrahost adaptation (a selective process) and (b) interhost transmission (a demographic process). The tree in (a) characterizes, for example, neuraminidase (NA) or hemagglutinin (HA) evolution in the influenza A virus, driven by positive selection; selection by host immunity is ongoing, whereas that from drug treatment may be intermittent. The tree in (b) represents interhost transmission and its associated bottleneck; for viruses that compartmentalize (such as human cytomegalovirus and HIV), similar patterns follow transmission to new compartments. The colored squares below the trees roughly indicate the diversity of the population through time. Intrahost adaptation may temporally decrease diversity owing to genetic hitchhiking, though single snapshots may not reflect varying temporal levels of diversity. During interhost transmission, diversity decreases owing to the associated bottleneck but then may quickly recover in the new host.

as rigorously defining the term ‘generation’ for virus populations, and subsequently confirming that the per-generation mutation rate is on the order of the coalescent timescale c_N , a prerequisite for the use of any coalescent approach. Finally, viruses with little or no recombination may be prone to clonal interference, and this should be explicitly accounted for in population models and resulting coalescents (see, for example, Strelkova and Lässig, 2012).

The processes that make viruses ideal candidates for MMCs can differ by scale (see Figure 3); for example, following transmission events, there are severe founder effects and potentially high recombination within the host (for example, HIV and human cytomegalovirus). Subsequent compartmentalization may introduce intrahost population structure through bottlenecks, colonization events, and extinction events (Renzette *et al.*, 2013). To date, it remains unclear how often MMCs fit the patterns of variation observed in intrahost versus interhost virus populations—but such comparisons are increasingly feasible (Box 1). Finally, periods of latency—temporary virus inactivation with cessation of reproduction—should be incorporated in such modeling, potentially as recurring mass extinction events (Taylor and Véber, 2009). Thus, multiple MMC models are a necessary but not final step toward addressing the various patterns observed at different scales of virus evolution (Table 1).

The large data sets often generated from viruses may also prove impractical for the likelihood-based methods commonly employed for MMCs. This limitation has partially been overcome by Eldon *et al.* (2015), who proposed an approximate likelihood method along with an approximate Bayesian computation approach based on the SFS to distinguish between the MMC and exponential population growth. Although both effects are expected to result in very similar SFSs,

characterized by an excess of singletons as compared with the Kingman coalescent, the bulk and tail of the SFS (that is, the higher-order frequency classes) typically differ, which can be assessed by approximate likelihood-ratio tests and approximate Bayes factors (Eldon *et al.*, 2015; see Box 1).

PURIFYING SELECTION AND LINKAGE IN VIRUS POPULATIONS

Modeling background selection

The joint modeling of the effects of genetic drift and positive selection, including in experimental evolution studies of virus populations, has improved our ability to distinguish adaptive from neutral mutations by minimizing the chance that the rapid fixation of a neutral allele is incorrectly interpreted as strong positive selection (Li *et al.*, 2012; Foll *et al.*, 2014; see Box 2). However, there is another process that must be incorporated if we are to fully understand mutation trajectories in virus populations: background selection.

BGS was originally proposed to explain patterns of reduced diversity in regions of low recombination—patterns that were previously suggested to be the signature of genetic hitchhiking around strongly beneficial mutations (see Begun and Aquadro, 1992 and Charlesworth *et al.*, 1993). It was argued that only neutral mutations present on the ‘least-loaded’ chromosomes—that is, those with the fewest deleterious mutations—have appreciable probabilities of reaching high frequencies or fixation. Kimura and Maruyama (1966) showed that the proportion of chromosomes belonging to the least-loaded class is

$$f_0 = \exp\left(-\frac{U}{2hs}\right), \quad (1)$$

Box 1 Future challenges in MMC models

In order to make multiple-merger coalescent (MMC) models biologically relevant for viruses, a number of important tasks remain:

1. Describe summary statistics that capture demographic features and processes when offspring distributions are highly skewed; such patterns will be required for large-scale inference in a computationally efficient (for example, approximate Bayesian) framework.
2. Better understand the behavior of commonly used summary statistics under such models, as done for F_{ST} by Eldon and Wakeley (2009), for commonly used divergence, site frequency spectrum, and linkage disequilibrium-based statistics.
3. Determine which MMCs are best suited for different scales of virus evolution (that is, intrahost, interhost, global); develop novel models if necessary.
4. Investigate the effects of violations of MMC assumptions (for example, overlapping generations, number of multiple-merger events) on inference.

Box 2 Future challenges in identifying the effects of BGS

As background selection (BGS) almost certainly affects inference in virus populations, accounting for its effects is critical. Future challenges include:

1. Account for BGS effects on the SFS by directly simulating weakly deleterious mutations, rather than by rescaling N_e .
2. Improve recombination maps for virus genomes.
3. Develop models combining the effects of nonequilibrium demography, positive selection, and BGS, ideally to allow for the joint estimation of all associated parameters.
4. Extend methods applied to other taxa to virus populations; for example, establishing a baseline of variation for use as a null expectation to estimate BGS levels across the genome, as done for *Drosophila*.

where U is the rate of mutation to a deleterious state, s is the selection coefficient against homozygous mutations and h is the dominance coefficient. For simplicity of modeling, h is usually set to 1 for viruses that carry a single copy of their genome in each virion, although polyploid effects could arise in the case of multiple virions infecting the same cell.

The least-loaded class, and thus genetic diversity in the presence of BGS, is dependent on the balance between the influx of deleterious mutations (occurring at rate U) and their removal by natural selection (according to the product hs). Assuming that offspring exclusively originate from the least-loaded class of individuals, Charlesworth *et al.* (1993) expressed the expected neutral diversity due to background selection as

$$\pi = 4 f_o N_e \mu, \quad (2)$$

where N_e is the effective population size and μ is the mutation rate. As BGS reduces the number of reproducing individuals, genetic drift increases, thus reducing genetic diversity and increasing stochasticity in allele trajectories. Furthermore, as only the genetic diversity segregating in the least-loaded class can be observed, population size inferred from measures of genetic diversity may be underestimated if BGS is not properly taken into account (Ewing and Jensen, 2016).

In the BGS model described above, strongly deleterious mutations are maintained in mutation-selection balance such that no skew in the SFS is expected, as rare variants are rapidly purged. Thus, a simple rescaling of N_e is often used as a proxy for the effects of BGS (see, for

example, Hudson and Kaplan, 1995; Zeng and Charlesworth, 2011; Prüfer *et al.*, 2012; Zeng, 2013). However, recent work has demonstrated that although this rescaling is appropriate for strongly deleterious mutations, it is largely inappropriate for weakly deleterious mutations that may segregate in the population. Figure 4 shows the skew in estimates of population size obtained using an approximate Bayesian computation approach when BGS is prevalent for two populations A and B that have split at time $\tau = 2N_e$ generations (reproduced from Ewing and Jensen, 2016). Furthermore, experimental work on the shape of the distribution of fitness effects in many organisms indicates that weakly deleterious mutations represent an important class (see, for example, Eyre-Walker and Keightley, 2007; Bank *et al.*, 2014). These mutations may act to skew the SFS toward rare alleles as they decrease the expected frequency of linked neutral mutations relative to neutral expectations. As subsequent demographic inference is based on the shape of this SFS, this effect should be properly accounted for by directly simulating weakly deleterious mutations rather than implementing a simple rescaling, as is common practice (Box 2). Though important analytical progress has been made in this area (see, for example, McVean and Charlesworth, 2000), simulations remain the best option for the nonequilibrium demographic models and alternative coalescents recommended here for inference in virus populations.

The effects of background selection on inference in virus populations

Efforts to estimate the impact of BGS in nonviral organisms have been well reported. One of the most notable examples is that of Comeron (2014), who estimated levels of BGS in *Drosophila melanogaster* based on the results of Hudson and Kaplan (1995) and Nordborg *et al.* (1996) using a high-definition recombination map, with results indicating strong effects across the genome. For viruses, similar efforts are in their infancy (Box 2), with the first attempt at such estimation in a virus reported recently by Renzette *et al.* (2016), utilizing the theoretical predictions of Innan and Stephan (2003). Interestingly, the full spectrum of recombination frequencies is available in viruses—from non-recombining (for example, most negative-sense RNA viruses), to re-assorting (for example, influenza viruses), to rarely recombining (for example, hepatitis C and West Nile viruses), to frequently recombining (for example, HIV) — offering a highly promising framework for comparative analyses investigating the pervasiveness of BGS effects (Chare *et al.*, 2003; Simon-Loriere and Holmes, 2011). Furthermore, given the high mutation rates and compact genomes of many viruses, evolutionary theory suggests effects at least equal to those seen in *Drosophila*.

In order to accomplish such inference, improved recombination maps for virus genomes will be important. With such maps in hand, and given the amenability of viruses to experimental perturbation, it may indeed be feasible to understand and account for BGS in models of virus evolution.

FUTURE DIRECTIONS

Given that skewed offspring distributions and pervasive linked selection are likely important factors influencing the inference of virus population parameters, it is important to note that multiple backward and forward simulation programs have recently been developed that make the modeling of these processes feasible (Hernandez, 2008; Messer, 2013; Thornton, 2014; Eldon *et al.*, 2015; Zhu *et al.*, 2015). This will allow researchers to directly simulate from parameter ranges relevant for their population of interest, developing a better intuition for the importance of these processes in shaping the observed genomic diversity. More concretely, the ability to now

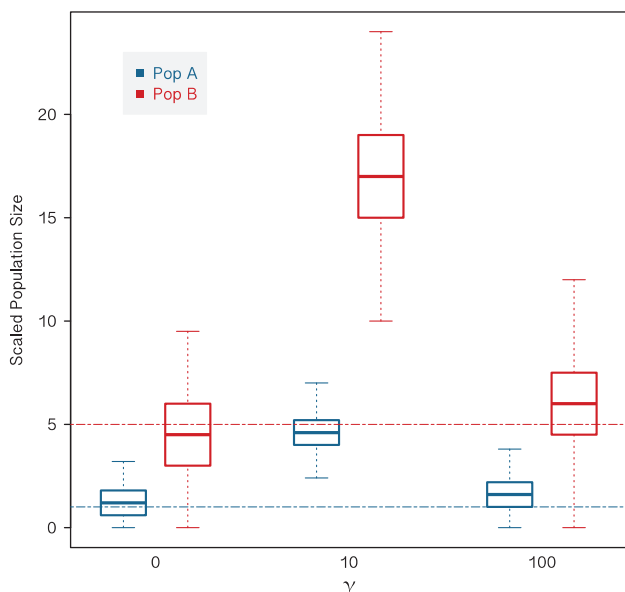


Figure 4 Bias in parameter inference at intermediate levels of BGS. Bias in parameter inference for different levels of BGS, redrawn from Ewing and Jensen (2016). Posterior densities from approximate Bayesian computation (ABC) inference for population size are shown. The strength of purifying selection is given as γ , where $\gamma=2N_e s$. Population A (Pop A) has a true scaled size of 1 (blue line), and population B (Pop B) a true scaled size of 5 (red line). Both population sizes are scaled relative to the size of the ancestral population. As shown, the greatest misinference occurs in the presence of weakly deleterious mutations and subsequent strong BGS effects.

simulate in a computationally efficient framework opens the possibility of directly implementing approximate Bayesian computation inference approaches under these models. Thus, by drawing mutations from a biologically realistic distribution of fitness effects and allowing offspring distributions to appropriately vary, it is now possible to reimplement common demographic estimation or genome scan approaches; these modified approaches would be based on more appropriate null expectations of the shape of the SFS, the extent of linkage disequilibrium, and the degree of population divergence.

DATA ARCHIVING

As a review article, no new data were processed, analyzed, or used directly.

CONFLICT OF INTEREST

The authors declare no conflict of interest.

ACKNOWLEDGEMENTS

We thank Bjarki Eldon for helpful suggestions during the early stages of this manuscript as well as Valeria Montano and three anonymous referees for later comments. This work was funded by the European Research Council (ERC) Starting Grant to JDJ, as well as Swiss National Science Foundation (FNS) grants to JDJ (31003A_159835) and SV (PMPDP3_158381).

Acevedo A, Brodsky L, Andino R (2014). Mutational and fitness landscapes of an RNA virus revealed through population sequencing. *Nature* **505**: 686–690.
Anderson RM, May RM (1991). *Infectious Diseases of Humans: Dynamics and Control*. Oxford University Press: Oxford.
Bank C, Hietpas RT, Wong A, Bolon DN, Jensen JD (2014). A Bayesian MCMC approach to assess the complete distribution of fitness effects of new mutations: uncovering the potential for adaptive walks in challenging environments. *Genetics* **196**: 841–852.

Basdevant A, Goldschmidt C (2008). Asymptotics of the allele frequency spectrum associated with the Bolthausen-Sznitman coalescent. *Electron J Probab* **13**: 486–512.
Begun DJ, Aquadro CF (1992). Levels of naturally occurring DNA polymorphism correlate with recombination rates in *D. melanogaster*. *Nature* **356**: 519–520.
Berestycki J, Berestycki N, Schweinsberg J (2007). Beta-coalescents and continuous stable random trees. *Ann Probab* **35**: 1835–1887.
Berestycki J, Berestycki N, Schweinsberg J (2008). Small-time behavior of beta coalescents. *Ann I H Poincaré-Pr* **44**: 214–238.
Bernet GP, Elena SF (2015). Distribution of mutational fitness effects and of epistasis in the 5' untranslated region of a plant RNA virus. *BMC Evol Biol* **15**: 274–287.
Birkner M, Blath J (2008). Computing likelihoods for coalescents with multiple collisions in the infinitely many sites model. *J Math Biol* **57**: 435–465.
Birkner M, Blath J, Eldon B (2013). An ancestral recombination graph for diploid populations with skewed offspring distribution. *Genetics* **193**: 255–290.
Blath J, Cronjäger MC, Eldon B, Hammer M (2016). The site-frequency spectrum associated with Ξ -coalescents. *Theor Popul Biol* **110**: 36–50.
Bolthausen E, Sznitman AS (1998). On Ruelle's probability cascades and an abstract cavity method. *Commun Math Phys* **197**: 247–276.
Chare R, Gould EA, Holmes EC (2003). Phylogenetic analysis reveals a low rate of homologous recombination in negative-sense RNA viruses. *J Gen Virol* **84**: 2691–2703.
Charlesworth B, Morgan MT, Charlesworth D (1993). The effect of deleterious mutations on neutral molecular variation. *Genetics* **134**: 1289–1303.
Cameron JM (2014). Background selection as a baseline for nucleotide variation across the *Drosophila* genome. *PLoS Genet* **10**: e1004434.
Cuevas JM, Geller R, Garijo R, López-Aldeguer J, Sanjuán R (2015). Extremely high mutation rate of HIV-1 in vivo. *PLoS Biol* **13**: e1002251.
Davies JL, Šimančík F, Lyngsø R, Mailund T, Hein J (2007). On recombination-induced multiple and simultaneous coalescent events. *Genetics* **177**: 2151–2160.
Der R, Epstein CL, Plotkin JB (2011). Generalized population models and the nature of genetic drift. *Theor Popul Biol* **80**: 80–99.
Donnelly P, Kurtz TG (1999). Particle representations for measure-valued population models. *Ann Probab* **27**: 166–205.
Eldon B, Birkner M, Blath J, Freund F (2015). Can the site-frequency spectrum distinguish exponential population growth from multiple-merger coalescents? *Genetics* **199**: 841–856.
Eldon B, Degnan JH (2012). Multiple merger gene genealogies in two-species: Monophyly, paraphyly, and polyphyly for two examples of Lambda coalescents. *Theor Popul Biol* **82**: 117–130.
Eldon B, Wakeley J (2006). Coalescent processes when the distribution of offspring number among individuals is highly skewed. *Genetics* **172**: 2621–2633.
Eldon B, Wakeley J (2008). Linkage disequilibrium under skewed offspring distribution among individuals in a population. *Genetics* **178**: 1517–1532.
Eldon B, Wakeley J (2009). Coalescence times and F_{st} under a skewed offspring distribution among individuals in a population. *Genetics* **181**: 615–629.
Ewens WJ (1979). Testing the generalized neutrality hypothesis. *Theor Popul Biol* **15**: 205–216.
Ewing GB, Jensen JD (2016). The consequences of not accounting for background selection in demographic inference. *Mol Ecol* **25**: 135–141.
Eyre-Walker A, Keightley PD (2007). The distribution of fitness effects of new mutations. *Nat Rev Genet* **8**: 610–618.
Ferrer-Admetlla A, Leuenberger C, Jensen JD, Wegmann D (2016). An approximate Markov model for the Wright-Fisher diffusion and its application to time series data. *Genetics* **203**: 831–846.
Foll M, Poh Y, Renzette N, Ferrer-Admetlla A, Bank C, Shim H *et al.* (2014). Influenza virus drug resistance: a time-sampled population genetic perspective. *PLoS Genet* **10**: e1004185.
Foll M, Shim H, Jensen JD (2015). WFABC: a Wright-Fisher ABC-based approach for inferring effective population sizes and selection coefficients from time-sampled data. *Mol Ecol Resour* **15**: 87–98.
Grenfell BT, Pybus OG, Gog JR, Wood JLN, Daly JM, Mumford JA *et al.* (2004). Unifying the epidemiological and evolutionary dynamics of pathogens. *Science* **303**: 327–332.
Gutiérrez S, Michalakis Y, Blanc S (2012). Virus population bottlenecks during within-host progression and host-to-host transmission. *Curr Opin Virol* **2**: 546–555.
Hedgecock D (1994a). Does variance in reproductive success limit effective population sizes of marine organisms? In: Beaumont AR (ed). *Genetics and Evolution of Aquatic Organisms*. Chapman & Hall: London. pp 122–133.
Hedgecock D (1994b). Population genetics of marine organisms. *US Globec News* **6**: 1–8.
Hernandez R (2008). A flexible forward simulator for populations subject to selection and demography. *Bioinformatics* **24**: 2786–2787.
Hudson RR, Kaplan NL (1995). Deleterious background selection with recombination. *Genetics* **141**: 1605–1617.
Huillet T, Möhle M (2011). Population genetics models with skewed fertilities: a forward and backward analysis. *Stoch Models* **27**: 521–554.
Innan H, Stephan W (2003). Distinguishing the hitchhiking and background selection models. *Genetics* **165**: 2307–2312.
Jiang L, Liu P, Bank C, Renzette N, Prachanronarong K, Yilmaz LS *et al.* (2016). A balance between inhibitor binding and substrate processing confers influenza drug resistance. *J Mol Biol* **428**: 538–523.
Joseph SB, Swanstrom R (2015). A fitness bottleneck in HIV-1 transmission. *Science* **345**: 136–173.
Kimura M, Maruyama T (1966). The mutational load with epistatic gene interactions in fitness. *Genetics* **54**: 1337–1351.

- Kingman JFC (1982). The coalescent. *Stoch Proc Applicat* **13**: 235–248.
- Knipe DM, Howley PM (2007). *Fields Virology* Vol 1, Lippincott Williams & Wilkins: Philadelphia.
- Lauring AS, Frydman J, Andino R (2013). The role of mutational robustness in RNA virus evolution. *Nat Rev Genet* **11**: 327–336.
- Li J, Li H, Jakobsson M, Li S, Sjödin P, Lascoux M (2012). Joint analysis of demography and selection in population genetics: where do we stand and where could we go? *Mol Ecol* **21**: 28–44.
- Li LM, Grassly NC, Fraser C (2014). Genomic analysis of emerging pathogens: methods, application and future trends. *Genome Biol* **15**: 541–550.
- Malaspinas A-S (2016). Methods to characterize selective sweeps using time serial samples: an ancient DNA perspective. *Mol Ecol* **25**: 24–41.
- Malaspinas A-S, Malaspinas O, Evans SN, Slatkin M (2012). Estimating allele age and selection coefficient from time-serial data. *Genetics* **192**: 599–607.
- McVean GAT, Charlesworth B (2000). The effects of Hill-Robertson interference between weakly selected mutations on patterns of molecular evolution and variation. *Genetics* **155**: 929–944.
- Messer PW (2013). SLiM: simulating evolution with selection and linkage. *Genetics* **194**: 1037–1039.
- Möhle M, Sagitov S (2001). A classification of coalescent processes for haploid exchangeable population models. *Ann Probab* **29**: 1547–1562.
- Moore CB, John M, James IR, Christiansen FT, Witt CS, Mallal SA (2002). Evidence of HIV-1 adaptation to HLA-restricted immune responses at a population level. *Science* **296**: 1439–1443.
- Moran PAP (1958). Random processes in genetics. *Math Proc Camb Phil Soc* **54**: 60–71.
- Neher RA, Hallatschek O (2013). Genealogies of rapidly adapting populations. *Proc Natl Acad Sci USA* **110**: 437–442.
- Neuhauser C, Krone SM (1997). The genealogy of samples in models with selection. *Genetics* **145**: 519–534.
- Nordborg M (1997). Structured coalescent processes on different time scales. *Genetics* **146**: 1501–1514.
- Nordborg M, Charlesworth B, Charlesworth D (1996). The effect of recombination on background selection. *Gen Res* **67**: 159–174.
- Pennings PS, Kryazhimskiy S, Wakeley J (2014). Loss and recovery of genetic diversity in adapting populations of HIV. *PLoS Genet* **10**: e1004000.
- Pitman J (1999). Coalescents with multiple collisions. *J Appl Probab* **27**: 1870–1902.
- Prüfer K, Munch K, Hellmann I, Akagi K, Miller JR, Walenz B *et al.* (2012). The bonobo genome compared with the chimpanzee and human genomes. *Nature* **486**: 527–531.
- Pybus OG, Rambaut A (2009). Evolutionary analysis of the dynamics of viral infectious disease. *Nat Rev Genet* **10**: 540–550.
- Renzette N, Gibson L, Bhattacharjee B, Fisher D, Schleiss MR, Jensen JD *et al.* (2013). Rapid intrahost evolution of human cytomegalovirus is shaped by demography and positive selection. *PLoS Genet* **9**: e1003735.
- Renzette N, Kowalik TF, Jensen JD (2016). On the relative roles of background selection and genetic hitchhiking in shaping human cytomegalovirus genetic diversity. *Mol Ecol* **25**: 403–413.
- Sagitov S (1999). The general coalescent with asynchronous mergers of ancestral lines. *J Appl Probab* **36**: 1116–1125.
- Sanjuán R (2010). Mutational fitness effects in RNA and single-stranded DNA viruses: common patterns revealed by site-directed mutagenesis studies. *Phil Trans R Soc B* **365**: 1975–1982.
- Schlub TE, Grimm AJ, Smyth RP, Cromer D, Chopra A, Mallal S *et al.* (2014). Fifteen to twenty percent of HIV substitution mutations are associated with recombination. *J Virol* **88**: 3837–3849.
- Schweinsberg J (2000). Coalescents with simultaneous multiple collisions. *Electron J Probab* **5**: 1–50.
- Schweinsberg J (2003). Coalescent processes obtained from supercritical Galton-Watson processes. *Stoch Proc Applicat* **106**: 107–139.
- Service SK, Blower SM (1995). HIV transmission in sexual networks: an empirical analysis. *Proc R Soc Lond B Biol Sci* **260**: 237–244.
- Simon-Lorieri E, Holmes EC (2011). Why do RNA viruses recombine? *Nat Rev Microbiol* **9**: 617–626.
- Steinrück M, Birkner M, Blath J (2013). Analysis of DNA sequence variation within marine species using Beta-coalescents. *Theor Popul Biol* **87**: 15–24.
- Strelkowa N, Lässig M (2012). Clonal interference in the evolution of influenza. *Genetics* **192**: 671–682.
- Taylor JE, Véber A (2009). Coalescent processes in subdivided populations subject to recurrent mass extinctions. *Electron J Probab* **14**: 242–288.
- Tebit DM, Arts EJ (2011). Tracking a century of global expansion and evolution of HIV to drive understanding and to combat disease. *Lancet Infect Dis* **11**: 45–46.
- Tellier A, Lemaire C (2014). Coalescence 2.0: a multiple branching of recent theoretical developments and their applications. *Mol Ecol* **23**: 2637–2652.
- Thornton KR (2014). A C++ template library for efficient forward-time population genetic simulation of large populations. *Genetics* **198**: 157–166.
- Wilkinson-Herbots HM (1998). Genealogy and subpopulation differentiation under various models of population structure. *J Math Biol* **37**: 535–585.
- Williamson EG, Slatkin M (1999). Using maximum likelihood to estimate population size from temporal change in allele frequencies. *Genetics* **152**: 755–761.
- Wright S (1931). Evolution in Mendelian populations. *Genetics* **16**: 97–159.
- Zeng K (2013). A coalescent model of background selection with recombination, demography and variation in selection coefficients. *Heredity* **100**: 363–371.
- Zeng K, Charlesworth B (2011). The joint effects of background selection and genetic recombination on local gene genealogies. *Genetics* **189**: 251–266.
- Zhu S, Degnan JH, Goldstein SJ, Eldon B (2015). Hybrid-Lambda: simulation of multiple merger and Kingman gene genealogies in species networks and species trees. *BMC Bioinformatics* **16**: 292–298.
- Zhu Y, Yongky A, Yin J (2009). Growth of an RNA virus in single cells reveals a broad fitness distribution. *Virology* **385**: 39–46.